Progress In Electromagnetics Research M, Vol. 102, 65–79, 2021

Marchenko Inversion of GPR Data for a 1D Dissipative Medium

Bingkun Yang* **and Evert Slob**

Abstract—Radar data collected on two sides of a horizontally dissipative layered medium are required to invert for the medium parameters. The two-sided reflection and transmission responses are reduced to two single-sided reflection responses. One is the measured dissipative medium response, and the other is the reflection response of the corresponding effectual medium, which has negative dissipation. Marchenko-type equations are solved using these two reflection responses. The obtained focusing functions in the dissipative and effectual media are used to invert for the permittivity and the permeability under the assumption of weak dissipation in reflection. Once these parameters are known, the travel times are used to estimate the layer thicknesses. Finally, the focusing functions are used to estimate the conductivity in each layer. The method does not require any model information and runs as a fully automated process. A numerical example shows that the method works well for a horizontally dissipative layered medium. Statistical analysis for several noise models shows that the method is robust at least up to 40 dB additive and multiplicative white noise.

1. INTRODUCTION

Ground Penetrating Radar (GPR) is an electromagnetic apparatus that is widely used in geophysical survey, especially in the geotechnical engineering survey or civil engineering application, because of its high resolution, low cost, and non-destructiveness [2]. To invert the medium parameters from the GPR data, the inverse problem needs to be solved.

There are two fundamentally different approaches for solving the GPR inverse problem: model-driven methods and data-driven methods. Model-driven methods are conventional schemes, which work with undersampled data. The medium parameters are estimated by updating a model, which provides the results to be the best-fit of the measured data [4, 21]. However, for model-driven inversion methods, essential issues that must be considered include solution existence, solution uniqueness, and instability of the solution process [16]. We need an initial model to start with model-driven methods and then minimize the so-called cost function or contrast function, which is the difference between the measured data and forward modeling data in each iteration. It is computationally expensive. If the initial model is not good enough, we cannot find the exact solution we need because multisolutions always occur in inverse problems. Moreover, the process of computing an inverse solution can be extremely unstable in that a small change in measurement can lead to an enormous change in the estimated model [6]. Commonly, we can stabilize the inversion process by imposing additional constraints (e.g., regularization) that bias the solution.

To solve the problems mentioned above, data-driven methods were proposed. When the data are properly sampled, the geophysical information is obtained from the measured data. The main feature of these methods is that the inverse problem is solved by processing steps and without model information, hence they find the solution to the inverse problem by solving a sequence of linear problems. The data-driven approaches require the data to be properly sampled in space and time because the medium

Received 9 February 2021, Accepted 2 April 2021, Scheduled 14 April 2021
* Corresponding author: Bingkun Yang (B.Yang@tudelft.nl).
The authors are with the Delft University of Technology, 2628 CN, Delft, The Netherlands.

parameters are extracted by filtering the data. It is a full waveform inversion method if the electric and magnetic parameters are obtained as a function of the subsurface position. Recently, some data-driven methods based on the Marchenko scheme have been proposed [11, 15, 17]. It was shown that the wave fields and focusing wave fields inside an unknown medium can be retrieved by solving a set of Marchenko-type equations [11, 19]. The Marchenko inversion scheme can be implemented as long as the Green's function or/and the focusing function are obtained because the local reflectivity or impedance can be obtained as a starting point for further inversion [11, 17]. The theory for 1D GPR inversion based on Marchenko redatuming has been derived for a lossless medium [11]. A 3D Marchenko redatuming method for dissipative acoustic media has been developed [13]. Van Der Neut & Fokkema presented a 1D Marchenko inversion in stretched space for the acoustic wave field [17]. Slob presented a theory using an integral equation that describes the electric focusing field inside the medium in terms of contrast source, then used the equation to invert the electric permittivity for a layer lossless model [15]. Yang & Slob presented a Marchenko inversion example of GPR data for a 1D layer dissipative medium but with a constant magnetic permeability [20].

In this paper, we present a Marchenko inversion theory of GPR data for the 1D blocky dissipative medium with variable conductivity, permittivity, and permeability. We assume that the medium is non-dispersive for the high-frequency GPR signal, which is reasonable for most GPR applications. It is worth noting that we need GPR data with different incidence angles for the method; the 3D electromagnetic wave fields in the 1D medium situation are required for our scheme. We need dissipative and equivalent effectual models to implement the Marchenko scheme in the dissipative medium. An effectual medium amplifies a propagating wave in the same way as a dissipative medium attenuates it [13]. Usually, we use an iterative scheme to solve the Marchenko equation and therefore require the earth impulse reflection response instead of the measured electric field. However, in a physical experiment, we can only measure the convolution of the impulse response with the signal that is emitted by the transmitter antenna. Additionally, GPR data are always contaminated by noise. We can obtain the impulse reflection response by the deconvolution process [1]. If we do not want to do the deconvolution first, we can follow the ideas applied in [8, 14] and use non-Neumann type solvers (e.g., LSQR) to solve the Marchenko equation. Here, we use the impulse reflection response as input and present the data-driven inversion scheme based on the Marchenko method in a dissipative medium. The 1D Marchenko inversion scheme presented in this paper provides a new way for any material testing where the material can be accessed for measurements at two opposite sides (e.g., building inspection). As a side application, it can be used in earth sciences on cross borehole data. In the 2D or 3D situation, we need multi-offset two-sided data, and the scheme must be adapted. The extension of the method to 2D and 3D is beyond the scope of this paper and open for investigation.

The paper is organized as follows: In Section 2, we briefly introduce the 3D electromagnetic wave field in a 1D dissipative medium. In Section 3, we derive field representations for the up- and down-going parts of the electromagnetic field based on reciprocity relations. In Section 4, we investigate the Marchenko method in a dissipative medium and an effectual medium. In Section 5, we show the way to use the two-sided measured reflection and transmission data to compute the up- and down-going electric fields received above the surface in the effectual medium. In Section 6, we present the way of obtaining the electric permittivity, magnetic permeability, conductivity, and the thickness of each layer from the focusing functions. In Section 7, we use a numerical example to illustrate the method. Then we investigate the effect of noisy data on the performance of the method.

2. ELECTROMAGNETIC PRINCIPLE

Here we propose to use two sets of single-sided Marchenko equations to obtain the electric and magnetic medium properties of a horizontally layered lossy medium directly from the measured data. The amplitude versus angle analysis in the $\tau - p$ domain shall be required to get the electric permittivity and permeability in our scheme. The 3D electromagnetic wave fields in 1D medium are required as input to implement the inversion scheme. It means that the Marchenko inversion scheme presented in this paper is a 3D scheme which works only for horizontally layered dissipative media. We use the vector $\mathbf{x} = (x, y, z)$ to denote the coordinate vector of a point in three-dimensional space, with the vertical axis pointing downward. The time coordinate is given by t. The vector wave field is

expressed as $\mathbf{P}(\mathbf{x}_T, z_r, z_s, t)$, where $\mathbf{P}$ can be electric field $\mathbf{E}$ or magnetic field $\mathbf{H}$; subscript T is used to indicate the horizontal vector; z_s is the source location; and z_r is the receiver location. We define the temporal Fourier transform of a function $\mathbf{P}(\mathbf{x}_T, z_r, z_s, t)$ to the space-frequency domain as $\hat{\mathbf{P}}(\mathbf{x}_T, z_r, z_s, \omega) = \int_{-\infty}^{\infty} \mathbf{P}(\mathbf{x}_T, z_r, z_s, t) e^{-i\omega t} dt$, abbreviated as $\hat{\mathbf{P}}$, where i denotes the imaginary unit, and ω denotes the angular frequency. A horizontally layered medium allows for carrying out a 2D spatial Fourier transformation as $\tilde{\mathbf{P}}(z_r, z_s, \mathbf{p}_T) = \int_{-\infty}^{\infty} \hat{\mathbf{P}}(\mathbf{x}_T, z_r, z_s, \omega) e^{i\omega \mathbf{x}_T \mathbf{p}_T} d\mathbf{x}_T$, abbreviated as $\tilde{\mathbf{P}}$, where $\mathbf{p}_T$ denotes the two components of the horizontal slowness vector and $\mathbf{p}_T \mathbf{x}_T = p_x x + p_y y$. Then the horizontal slowness p is given by $p = \sqrt{p_x^2 + p_y^2}$ in s/m. For a horizontally layered medium with interfaces at depth levels z_i, $i = 0, 1, 2, \ldots$, the sources are assumed to be located at depth level $z_s < 0$ and the receivers at depth level $z_r = 0$ such that $z_r > z_s$. The angles of incidence used in this paper are related to the angles in the air and hence for a wave field in the air with incidence angle φ and horizontal slowness p are related through $p = \sin\varphi / c_0$ with c_0 being the velocity in the air. We perform the derivations in $p - \omega$ domain in which the wave field shall be written by $\tilde{P}(z_r, z_s, p)$, and analyse the resulting equations in the $\tau - p$ domain in which the wave field shall be written by $P(z_r, z_s, p, \tau)$, where τ is intercept time. The up-down decomposition electromagnetic wave field is carried out in the slowness-frequency domain because it can be easily carried out for each slowness and each frequency separately.

Consider an $(N+1)$-layered model, the depth level of a reflector is denoted by $z_n\,(\mathrm{m}), n = 0, 1, 2, \ldots, N+1$, and each layer is homogeneous and isotropic. We only consider non-dispersive parameters, which means that permittivity, permeability, and conductivity are frequency-independent quantities, and all of them are real values [5]. The antenna frequency we consider in this paper is above 100 MHz. In the layer n, the electric permittivity is denoted by $\varepsilon_n\,(\mathrm{F/m})$; the electric conductivity is denoted by $\sigma_n\,(\mathrm{S/m})$, the magnetic permeability is denoted by $\mu_n\,(\mathrm{H/m})$; the impedance is given by $Z_n = \sqrt{\mu_n/\varepsilon_n}$; the admittance is given by $Y_n = \sqrt{\varepsilon_n/\mu_n}$; the layer thickness is denoted by $d_n\,(\mathrm{m})$, given by $d_n = z_n - z_{n-1}$.

From Maxwell's equations, we can get two independent sets of scalar equations. One set describes the so-called Transverse Electric (TE) mode, which does not depend on the vertical component of the electric field. The other set describes the so-called Transverse Magnetic (TM) mode, which does not depend on the vertical component of the magnetic field [9]. Since the inverse problem can be solved with either mode, here we introduce the TE mode field as follows:

$$\partial_z \begin{bmatrix} \tilde{E} \\ \tilde{H} \end{bmatrix} + \begin{bmatrix} 0 & \zeta \\ \zeta^{-1}(\omega^2 p^2 + \eta\zeta) & 0 \end{bmatrix} \begin{bmatrix} \tilde{E} \\ \tilde{H} \end{bmatrix} = \begin{bmatrix} 0 \\ \tilde{J}^e \end{bmatrix}, \tag{1}$$

where $\tilde{E} = \omega p_y \tilde{E}_x - \omega p_x \tilde{E}_y$, $\tilde{H} = \omega p_x \tilde{H}_x + \omega p_x \tilde{H}_y$; ζ denotes the transverse magnetic resistance given by $\zeta = i\omega\mu\ (\Omega/\mathrm{m})$; η denotes a generalized conductivity given by $\eta = \sigma + i\omega\varepsilon\,(\mathrm{S/m})$; superscript t denotes the matrix transposition; and $\tilde{J}^e$ denotes the electric current source given by $\tilde{J}^e = \omega p_x \tilde{J}_y^e - \omega p_y \tilde{J}_x^e$.

At any location, we can write the electric field and magnetic field of the TE model as the sum of up- and down-going wave fields [10]: $\tilde{E} = \tilde{E}^+ + \tilde{E}^-$ and $\tilde{H} = \tilde{H}^+ + \tilde{H}^-$, where down-going is indicated with superscript $+$ and up-going with superscript $-$. The vertical wave number, Γ, in the dissipative medium is given by $\Gamma = \sqrt{\omega^2 p^2 + \zeta\eta}$, which can be written as $\Gamma = \alpha + \beta i$, where α denotes the attenuation coefficient, and β denotes the phase coefficient. For GPR applications, we use a high central frequency larger than 100 MHz. The electromagnetic wave field starts in the air, and propagating waves have a maximum p-value equal to $\sqrt{\varepsilon_0\mu_0}$, in which the incidence angle $\varphi = \pi/2$. We also know that $\varepsilon_0\mu_0 < \varepsilon_n\mu_n$ for any $n > 0$. Hence, we can always choose p-values that satisfy $|\sigma\mu / [(\varepsilon\mu - p^2)\,\omega]| \ll 1$. Taking the Taylor series expansion around the point $|\sigma\mu / [(\varepsilon\mu - p^2)\,\omega]| = 0$, then Γ can be written as

$$\Gamma = i\omega\sqrt{\varepsilon\mu - p^2} \left\{ 1 + \sum_{n=1}^{\infty} \left[\left(\frac{-i\sigma\mu}{\omega\varepsilon\mu - \omega p^2} \right)^n \prod_{k=1}^{k=n} \frac{3-2k}{2k} \right] \right\}. \tag{2}$$

Truncate this series after the second term, then α and β can be approximately given by

$$\alpha = \sigma\mu \left(2\sqrt{\varepsilon\mu - p^2} \right)^{-1}, \quad \text{and} \quad \beta = \omega\sqrt{\varepsilon\mu - p^2}. \tag{3}$$

To implement the Marchenko redatuming scheme in the lossy model, we need to define two media related to each other. One is a dissipative (physical) medium, and the other one is an effectual (non-physical) medium. The effectual medium is the same as the dissipative medium, but with negative conductivity such that the wave field gains strength on its propagation path. The electric and magnetic wave fields in the corresponding effectual medium are denoted as $\mathscr{E}$ and $\mathscr{H}$, respectively. The vertical wave number in effectual medium shall be $-\Gamma^*$, which is equal to $-\alpha+\beta i$.

3. RECIPROCITY THEOREM FOR ONE-WAY ELECTROMAGNETIC WAVE FIELDS

The reciprocity theorem relates two non-identical electromagnetic wave fields labeled state A and state B (indicated by subscripts A and B). The representations are derived in the slowness-frequency domain but are valid in other domains as well. We apply reciprocity to a horizontally infinite but vertically finite domain [18]. The wave fields are evaluated at two depth levels, the receiver level z_r and the focusing level z_f. The wave fields propagate inside the investigation domain $\mathbb{D}$ and are decomposed into down-going and up-going components. We start with the time convolution type reciprocity theorem for one-way wave fields without a source inside the investigation domain $\mathbb{D}$. These wave fields are propagating forward in time which is given by [18]

$$\left[\tilde{E}_B^+\tilde{H}_A^- + \tilde{E}_B^-\tilde{H}_A^+\right]|_{z_r} = -\left[\tilde{E}_A^+\tilde{H}_B^- + \tilde{E}_A^-\tilde{H}_B^+\right]|_{z_f}. \tag{4}$$

Because all wave field quantities are expressed in the slowness-frequency domain, the multiplications in Eq. (4) are equivalent to convolutions in the time-space domain. Eq. (4) is valid when the medium parameters between the surface level z_r and focusing level z_f are the same in both state A and state B. However, the medium parameters of the two states can be different from each other outside of the investigation domain $\mathbb{D}$.

In order to get an analogous reciprocity relationship of the time correlation type for one-way wave fields in the dissipative medium, we need to eliminate the influence of the conduction in the investigation domain $\mathbb{D}$. According to [18], one of the states should be in the dissipative medium and the other one in the effectual medium. Here, we assume that state A is in the dissipative medium, while state B is in the effectual medium. The medium parameters outside of the domain $\mathbb{D}$ in both states can be any kinds of media. In this situation, the correlation type reciprocity relation of one-way electromagnetic wave fields is given by [18]

$$\left[\left(\tilde{H}_A^+\right)^* \tilde{\mathscr{E}}_B^+ + \left(\tilde{H}_A^-\right)^* \tilde{\mathscr{E}}_B^-\right]|_{z_r} = \left[\left(\tilde{E}_A^+\right)^* \tilde{\mathscr{H}}_B^+ + \left(\tilde{E}_A^-\right)^* \tilde{\mathscr{H}}_B^-\right]|_{z_f}. \tag{5}$$

Here, the superscript * denotes complex conjugation, being equivalent to time reversal in the time-space domain. Eq. (5) relates wave fields that propagate forward in time to wave fields that propagate backward in time. Hence, the multiplications in Eq. (5) are cross-correlations in the time-space domain. Sources exist only outside of the investigation domain $\mathbb{D}$ in Eqs. (4)–(5).

4. METHOD

The focusing functions in the dissipative medium and effectual medium are required to implement the inversion scheme, and we can obtain these two sets of the focusing functions analogously. Here, we only show how to get the focusing function in the dissipative medium in detail. To obtain the convolution type Marchenko equation, we take the medium in state A identical to the physical medium above the focusing level z_f and reflection-free below this level. For state B, we choose the physical medium. To get the correlation type Marchenko equation, we take the medium in state A as a truncated medium like we set for the convolution type Marchenko equation and choose the effectual medium for state B. For the sake of narrative convenience, we derive the formulas in the slowness-frequency domain, but they can be transformed to other domains without losing their validity. Then in state A, at the receiver lever, we define the magnetic field as the focusing wave field $\tilde{f}_1(z_r, z_f, p)$ and the initial down-going focusing function is a unit amplitude impulse. The corresponding electric field focuses just below z_f. At the receiver level, the up- and down-going magnetic fields in state A are given by $\tilde{f}_1^{\pm}(z_r, z_f, p)$. Under this

assumption, the last event of the up-going focusing function would be the local reflection coefficient of the focusing point with 2 times decay from the focusing point to the receiver point [12, 13]. Then based on the focusing condition, the up- and down-going electric wave fields at the focusing level z_f are given by

$$\tilde{E}_A^+(z_f, z_f, p) = \tilde{A}(z_f, z_r, p)\, e^{i\omega t_d(z_r, z_f, p)}, \quad \tilde{E}_A^-(z_f, z_f, p) = 0, \tag{6}$$

where $\tilde{A}(z_f, z_r, p)$ denotes the direct arrival of the transmission response from z_r to z_f, and $t_d(z_r, z_f, p)$ denotes the direct travel time from acquisition surface z_r to focusing point z_f which is given by $t_d(z_r, z_f, p) = \sum_{m=0}^{N} d_m q_m$, $q_m = \sqrt{\mu_m \varepsilon_m - p^2}$. For GPR applications, it is reasonable to suppose that the attenuation is frequency independent (see Eq. (3)), then $\tilde{E}_A^+(z_f, z_f, p)$ only contains one event. Its amplitude is equal to the transmission amplitude from z_f to z_r. In state B, we place an electric current source at the level z_s and receiver at the level z_r such that the up- and down-going electric wave fields at the receiver level are given by $\tilde{E}_B^{\pm}(z_r, z_s, p) = \tilde{E}^{\pm}(z_r, z_s, p)$ in the dissipative medium or $\tilde{\mathscr{E}}_B^{\pm}(z_r, z_s, p) = \tilde{\mathscr{E}}^{\pm}(z_r, z_s, p)$ in the effectual medium. In the next section, we investigate how to compute $\tilde{\mathscr{E}}^{\pm}(z_r, z_s, p)$ from the two-sided data. At the focusing level, we refer to the wave fields in state B as the up- and down-going magnetic wave fields given by $\tilde{H}_B^{\pm}(z_f, z_s, p) = \tilde{H}^{\pm}(z_f, z_s, p)$ in the dissipative medium and $\tilde{\mathscr{H}}_B^{\pm}(z_f, z_s, p) = \tilde{\mathscr{H}}^{\pm}(z_f, z_s, p)$ in the effectual medium. Substituting these choices into Eqs. (4) and (5), we obtain:

$$\tilde{E}_A^+(z_f, z_f, p)\, \tilde{H}^-(z_f, z_s, p) = -\left[\tilde{E}^+(z_r, z_s, p)\, \tilde{f}_1^-(z_r, z_f, p) + \tilde{E}^-(z_r, z_s, p)\, \tilde{f}_1^+(z_r, z_f, p)\right], \tag{7}$$

$$(\tilde{E}_A^+(z_f, z_f, p))^* \tilde{\mathscr{H}}^+(z_f, z_s, p) = \tilde{\mathscr{E}}^+(z_r, z_s, p) \left(\tilde{f}_1^+(z_r, z_f, p)\right)^* + \tilde{\mathscr{E}}^-(z_r, z_s, p) \left(\tilde{f}_1^-(z_r, z_f, p)\right)^*. \tag{8}$$

If we interchange actual and effectual media and use a unit amplitude impulse as the initial down-going focusing function, we obtain similar equations for the other pair of up- and down-going parts of the magnetic field.

$$\tilde{\mathscr{E}}_A^+(z_f, z_f, p)\, \tilde{\mathscr{H}}^-(z_f, z_s, p) = -\left[\tilde{\mathscr{E}}^+(z_r, z_s, p)\, \tilde{\mathfrak{f}}_1^-(z_r, z_f, p) + \tilde{\mathscr{E}}^-(z_r, z_s, p)\, \tilde{\mathfrak{f}}_1^+(z_r, z_f, p)\right], \tag{9}$$

$$(\tilde{\mathscr{E}}_A^+(z_f, z_f, p))^* \tilde{H}^+(z_f, z_s, p) = \tilde{E}^+(z_r, z_s, p) \left(\tilde{\mathfrak{f}}_1^+(z_r, z_f, p)\right)^* + \tilde{E}^-(z_r, z_s, p) \left(\tilde{\mathfrak{f}}_1^-(z_r, z_f, p)\right)^*, \tag{10}$$

where $\tilde{\mathscr{E}}_A^+(z_f, z_f, p)$ denotes the transmission electric field at the focusing level, which satisfies the focusing condition in the effectual medium, and $\mathfrak{f}_1$ denotes the magnetic focusing wave field in the effectual medium. The electric counterpart of that focuses just below z_f.

Equations (7) and (10) can be seen as the magnetic wave fields at the receiver level z_f retrieval equations for the scaled up- and down-going wave fields in the dissipative medium. Eqs. (8) and (9) can be seen as the magnetic wave fields retrieval representations for the up- and down-going wave fields in the effectual medium. To find the focusing functions in the dissipative and effectual media, we can eliminate all of the left-hand sides of Eqs. (7)–(10). In the time domain, we can separate the magnetic fields and the focusing fields. Here, we present how to solve Eqs. (7)–(8). The impulse reflection response of the layered medium at the receiver level can be given by $\tilde{R}(z_r, z_r, p) = \tilde{E}^-(z_r, z_s, p) / \tilde{E}^+(z_r, z_s, p)$ in the dissipative medium or $\tilde{\mathscr{R}}(z_r, z_r, p) = \tilde{\mathscr{E}}^-(z_r, z_s, p) / \tilde{\mathscr{E}}^+(z_r, z_s, p)$ in the effectual medium [1]. Doing the deconvolution gives us

$$\tilde{E}_A^+(z_f, z_f, p)\, \tilde{G}^-(z_f, z_r, p) = -\tilde{f}_1^-(z_r, z_f, p) - \tilde{R}(z_r, z_r, p)\, \tilde{f}_1^+(z_r, z_f, p), \tag{11}$$

$$\tilde{E}_A^+(z_f, z_f, p)\, \tilde{\mathscr{G}}^+(z_f, z_r, p) = \left(\tilde{f}_1^+(z_r, z_f, p)\right)^* + \tilde{\mathscr{R}}(z_r, z_r, p) \left(\tilde{f}_1^-(z_r, z_f, p)\right)^*. \tag{12}$$

where $\tilde{G}^-(z_f, z_r, p)$ denotes the up-going parts of the Green's function in the physical medium observed at z_f and generated by a down-going source at z_r, given by $\tilde{G}^-(z_f, z_r, p) = \tilde{H}^-(z_f, z_s, p) / \tilde{E}^+(z_r, z_s, p)$ and $\tilde{\mathscr{G}}^+(z_f, z_r, p)$ denotes the down-going parts of the Green's function in the effectual medium observed at z_f and generated by a down-going source at z_r, given by $\tilde{\mathscr{G}}^+(z_f, z_r, p) = \tilde{\mathscr{H}}^+(z_f, z_s, p) / \tilde{\mathscr{E}}^+(z_r, z_s, p)$.

In state A, we let the focusing point be located just below z_f and focus the wave field at $\tau = 0$, so the first arrival should not arrive at the focus point before zero time. It means that we inject the initial down-going focusing wave field at time $\tau = -t_d(z_r, z_f, p)$. This implies that the focusing wave field is zero before the negative travel time from the acquisition surface to the focus point. That bounds the time duration at negative times. Then the first arrival can reflect from the focusing point and return to the surface. After that arrival, nothing is allowed to arrive later; otherwise, the extra events would lead to a new reflection event, and there would be more than one event at the focusing level. That bounds the time duration at positive times. So the focusing wave fields do not exist for $|\tau| > t_d(z_r, z_f, p)$. In state B, we let the source be excited at $\tau = 0$, and the first arrival from the source level to the focusing point is recorded in $z = z_f$ at $\tau = t_d(z_f, z_s, p)$. Therefore, before $\tau = t_d(z_f, z_s, p)$, the magnetic wave fields of the left-hand sides of the Eqs. (11)–(12) are zero. Transforming Eqs. (11)–(12) to $\tau - p$ domain, we can write the down-going part of the focusing wave field as

$$f_1^+(z_r, z_f, p, \tau) = \delta(\tau + t_d(z_f, z_r, p)) + f_{1m}^+(z_r, z_f, p, \tau), \tag{13}$$

where f_{1m}^+ represents the coda following the initial down-going focusing event δ.

We assume that the medium parameters are real value and frequency-independent quantities. It means that the wave velocity does not change with the frequency in each layer. When we solve the focusing functions in the $\tau - p$ domain, we can always pick the last event of the up-going focusing function without overlapping with the Green's function even if we consider the data with a finite frequency bandwidth. Substitute Eq. (13) into the $\tau - p$ domain of Eqs. (11) and (12), and apply a time window $|\tau| \leq t_d(z_r, z_f, p)$ to Eq. (11) and a time window $|\tau| < t_d(z_r, z_f, p)$ to Eq. (12). We get the coupled Marchenko equations:

$$\int_{t'=-t_d}^{\tau} \left[R\left(z_r, z_r, p, \tau - t'\right) f_{1m}^+\left(z_r, z_f, p, t'\right)\right] dt' + f_1^-(z_r, z_f, p, \tau) = -R(z_r, z_s, p, \tau + t_d(z_r, z_f, p)) \tag{14}$$

$$f_{1m}^+(z_r, z_f, p, \tau) + \int_{t'=-\tau}^{t_d} \left[\mathscr{R}\left(z_r, z_r, p, \tau + t'\right) f_1^-\left(z_r, z_f, p, t'\right)\right] dt' = 0. \tag{15}$$

Note that the initial down-going focusing function does not play a role in Eq. (15) because the time window $|\tau| < t_d(z_r, z_f, p)$ excludes the time instant $t_d(z_r, z_f, p)$. If the impulse reflection response in Eqs. (14)–(15) is convolved with a zero-phase filter function W that has finite bandwidth, the focusing functions shall be convolved with the same zero-phase function W. Then the time window we used above would become $|\tau| < t_d(z_r, z_f, p) + t_w$, where t_w denotes half the time duration of the wavelet W. When the medium is dissipative, the Neumann-type iterative solution for Eqs. (14) and (15) may diverge and fail to yield a solution [3]. However, non-Neumann type solvers (e.g., LSQR) can always converge to a solution with a monotonically decreasing residual [3, 7]. We choose LSQR to solve Eqs. (14) and (15). Note that the attenuation in our model cannot be too strong. On the one hand, we require that waves can propagate across the medium under investigation so that the transmission response can be measured. Nevertheless, the effect of attenuation on propagation can be significant and cannot be ignored. On the other hand, when the attenuation is strong, the LSQR method does not guarantee to obtain a solution that shall be closer to the true one than other methods. We refer to [3] for further details.

5. UP- AND DOWN-GOING WAVE FIELDS IN THE EFFECTUAL MEDIUM

To solve Eqs. (14) and (15), the impulse reflection responses in the dissipative medium and effectual medium are needed. To obtain the impulse reflection response in the effectual medium, we need two sets of data collected in the physical dissipative medium [13]. One set is that we put a source in the upper half space at z_s and observed in the upper half space at z_r and the lower half space at z_m. The other set is that we put a source in the lower half space at z_{s_m} and observed at z_r and z_m. We then assume that, in the effectual medium, a source is deployed in the upper half space at z_s and observed at z_r and z_m. We also assume that the areas above the interface z_r in both dissipative medium and effectual medium are air, which are lossless media, so that the wave fields from the source level z_s to the receiver level z_r in the dissipative medium and effectual medium are the same (i.e., $\tilde{E}^+(z_r, z_s, p) = \tilde{\mathscr{E}}^+(z_r, z_s, p)$).

Substituting the wave fields above into the equation for reciprocity theorems of the time-correlation type (Eq. (5)), we find that the up-going wave fields in the effectual medium are given by

$$\tilde{\mathscr{E}}^{-}(z_r, z_s, p) = \frac{\left[\tilde{E}^{+}(z_m, z_{s_m}, p)\tilde{H}^{+}(z_r, z_s, p)\right]^{*} \tilde{E}^{+}(z_r, z_s, p)}{\left[\tilde{H}^{-}(z_r, z_s, p)\tilde{E}^{+}(z_m, z_{s_m}, p)\right]^{*} - \left[\tilde{E}^{+}(z_m, z_s, p)\tilde{H}^{-}(z_r, z_{s_m}, p)\right]^{*}}. \tag{16}$$

Now we have computed the up- and down-going components of the electric fields in the dissipative medium and the effectual medium from the measured data.

6. RECURSIVE INVERSION

In our scheme, the last event of the up-going focusing function is what we need to implement the inversion scheme. The intercept time of that event is the time where we find it plus $t_d(z_f, z_r, p)$. For a layer model, we can extract the local reflection strength of the reflector, jump from layer to layer, and do not need to do it for every time step.

In Section 2, we assume that $|\sigma\mu/\left(\varepsilon\mu - p^2\right)\omega| \ll 1$ so that we can take the zero and first-order terms in the Taylor series expansion of Γ and make the approximation represented by Eq. (3). The reflection coefficient is then automatically independent of frequency. In the horizontal intercept-time domain, the TE mode local reflection coefficient of the reflector at the depth level z_n is given by [11]

$$r_n(\varepsilon, \mu, p) = \frac{\mu_{n+1}\sqrt{\mu_n\varepsilon_n - p^2} - \mu_n\sqrt{\mu_{n+1}\varepsilon_{n+1} - p^2}}{\mu_{n+1}\sqrt{\mu_n\varepsilon_n - p^2} + \mu_n\sqrt{\mu_{n+1}\varepsilon_{n+1} - p^2}}. \tag{17}$$

As we show in Section 4, in the dissipative medium, the last event of the up-going focusing function would be the local reflection coefficient of the focusing point with 2 times decay from the focusing point to the receiver point. Similarly, in the effectual medium, the last event of the up-going focusing function would be the local reflection coefficient of the focusing point with 2 times of growth from the focusing point to the receiver point. Then the last event of the up-going focusing function in the dissipative medium and the effectual medium at focus level z_n, with the various p values, can be written as

$$f_1^{-}\left(z_r, z_n, p, \tau = t_d\right) = r_n\left(\varepsilon, \mu, p\right) \prod_{k=1}^{n} e^{-2\alpha_k d_k}, \quad \text{and} \quad \mathfrak{f}_1^{-}\left(z_r, z_n, p, \tau = t_d\right) = r_n\left(\varepsilon, \mu, p\right) \prod_{k=1}^{n} e^{2\alpha_k d_k}, \tag{18}$$

where α_k denotes the attenuation coefficient of the medium from level z_{k-1} to z_k, and r_n denotes the local reflection coefficient of the reflector at the focusing level z_n in the lossless medium. Then the local reflection coefficient $r_n\left(\varepsilon, \mu, p\right)$ in the equivalent lossless medium can be given by [13]

$$r_n\left(\varepsilon, \mu, p\right) = \operatorname{sign}\left(f_1^{-}\left(z_r, z_n, p, \tau = t_d\right)\right) \sqrt{f_1^{-}\left(z_r, z_n, p, \tau = t_d\right) \mathfrak{f}_1^{-}\left(z_r, z_n, p, \tau = t_d\right)}. \tag{19}$$

All local reflection coefficients in the equivalent lossless medium are obtained independently from each other. For the parameters, we start in the air with $n = 0$, where the receivers are present, and work our way down into the layered medium. Starting by assuming that we know the medium parameters in the air, $\varepsilon_r = 1$, $\mu_r = 1$, and we find the solution recursively for the layer below an interface. Once we have the electric permittivity, magnetic permeability, and the normal incidence intercept-time, we can find the solution for the conductivity and thickness of each layer. Notice that the two unknowns, magnetic permeability μ and electric permittivity ε, are constrained by just one Eq. (17), so we need to use different p-values to find the solutions.

When the incidence angle is zero ($p = 0$), Eq. (17) leads to the recursive estimate

$$Y_{n+1} = \left(\frac{1 - r_n(\varepsilon, \mu, 0)}{1 + r_n(\varepsilon, \mu, 0)}\right) Y_n, \tag{20}$$

where Y_n denotes the admittance of layer n. The known value of Y_0 is the admittance of free space, which is used to initialize the recursive solution. When the incidence angle is non-zero, the

magnetic permeability can be expressed with the aid of Eq. (17) for discrete values of p, $p_m = m\Delta p$, $m = 1, 2, \ldots, M$, as

$$\mu_{n+1} = \sqrt{\sum_{m=1}^{M} p_m^2 \sum_{m=1}^{M} \left[Y_{n+1}^2 - \left(\frac{1 - r_n(\varepsilon, \mu, p_m)}{1 + r_n(\varepsilon, \mu, p_m)} \right)^2 \left(Y_n^2 - p_m^2 \frac{1}{\mu_n^2} \right) \right]^{-1}}. \tag{21}$$

We infer the magnetic permeability μ using the various ray-parameters p based on Eq. (21). Once we have the magnetic permeability, we can infer the electric permittivity ε, the conductivity σ, and the thickness d by using only $p = 0$. From Eq. (21), we find μ_{n+1} for layer $n + 1$, then we use the value of μ_{n+1} in Y_{n+1}^2 from Eq. (20) to find ε_{n+1} for layer $n + 1$. Once we have the electric permittivity ε and permeability μ for each layer, we know the propagation velocities inside each layer and can transform the one-way vertical travel time for $p = 0$ to depth.

Until now, we have the up-going focusing functions in the dissipative medium and effectual medium, the travel time, and ε for each layer. The conductivity σ is found as follows. When $p = 0$, we use the values for permittivity and permeability into Eq. (20) which results in

$$f_1^- (z_r, z_n, 0, \tau = t_d) = r_n(\varepsilon, \mu, 0) \prod_{k=1}^{n} e^{-\frac{\sigma_k t_k}{\varepsilon_k}}, \quad \text{and} \quad \mathfrak{f}_1^- (z_r, z_n, 0, \tau = t_d) = r_n(\varepsilon, \mu, 0) \prod_{k=1}^{n} e^{\frac{\sigma_k t_k}{\varepsilon_k}}, \tag{22}$$

where t_k denotes the one-way vertical travel time from level z_{k-1} to z_k, given by $t_k = (z_k - z_{k-1})/c_k$, and c_k denotes the velocity of the layer k given by $c_k = 1/\sqrt{\mu_k \varepsilon_k}$. The one-way vertical travel time t_k for each layer can be extracted from the peak values of the up-going focusing function in Eq. (22), because one peak value of the up-going focusing function is corresponding to a reflector. We divide $\mathfrak{f}_1^-$ by f_1^- and take logarithm of both sides, which gives

$$P_n = \ln \left\{ \frac{\mathfrak{f}_1^- (z_r, z_n, 0, \tau = t_d)}{f_1^- (z_r, z_n, 0, \tau = t_d)} \right\}, \tag{23}$$

where $P_n = \sum_{k=0}^{n} 2\frac{\sigma_k t_k}{\varepsilon_k}$. The conductivity for the $(n + 1)$th layer is then given by

$$\sigma_{n+1} = \frac{(P_{n+1} - P_n)\, \varepsilon_{k+1}}{2t_{k+1}}. \tag{24}$$

With this last step, the full waveform inversion is complete.

In practice, we do not know the medium parameters. Thus, there is no measure for the quality of the inversion result. We use the same error criterion that is used in model-driven inversion. In the $\tau - p$ domain, we suggest the global normalized root-mean-square error (GRSE) to estimate the error between the data, $e_{p,i}$, obtained from forward modelling using the retrieved medium parameters and the measured data $E_{p,i}$, where $e_{p,i}$ and $E_{p,i}$ can be the reflection data or transmission data. The GRSE is given by

$$GRSE_{n_a, n_t} = \sqrt{\sum_{p=0}^{n_a} \sum_{i=1}^{n_t} (e_{p,i} - E_{p,i})^2 \sum_{p=0}^{n_a} \sum_{i=1}^{n_t} E_{p,i}^{-2}}, \tag{25}$$

where n_t denotes the number of samples in a specific time window, and n_a denotes the number of incidence angles used.

7. NUMERICAL RESULTS

7.1. Model without Noise

To illustrate the Marchenko inversion method in a dissipative medium, we use a Ricker wavelet with 250 MHz center frequency, f_c. The model consists of a layered medium with 7 reflecting interfaces below the upper half space. The layered model is given in Table 1. The attenuation for amplitude α_A for a vertically travelling wave is defined as $\alpha_A = 10\log_{10} e^{\alpha}$, which is given in the material parameters

Table 1. Model parameters.

d (m)	ε_r	μ_r	σ (mS/m)	$\sigma/(\omega_c\varepsilon)$	α_A (dB/m)
0.76	1.00	1.00	0.00	0.000	0.000
0.75	3.50	1.00	3.30	0.067	1.443
0.27	13.1	1.10	10.2	0.056	2.418
0.30	16.3	1.00	18.9	0.083	3.830
0.34	12.8	1.10	13.2	0.074	3.166
0.28	14.8	1.00	9.30	0.045	1.978
0.29	11.1	1.10	9.00	0.058	2.318
0.76	14.0	1.10	6.30	0.032	1.445

table in dB/m together with the value of $\sigma/(\omega_c\varepsilon)$, where $\omega_c = 2\pi f_c$. Note again that we assume that $|\sigma\mu/[(\varepsilon\mu - p^2)\,\omega]| \ll 1$, which means that $\varepsilon\mu$ should be much larger than p^2. As we all know, $\sin\varphi$ is a monotonically increasing function between 0 and 90°, which means that p^2 is a monotonically increasing function on the interval as well. To ensure that $|\sigma\mu[(\varepsilon\mu - p^2)\,\omega]| \ll 1$ and consider that we can take the average of multiple values to reduce the inversion error of the magnetic permeability value in Eq. (21), we take 35 different incidence angles relative to the vertical axis from 0° to 34° with increments of 1°. We show the process to implement Marchenko inversion scheme in this model step by step.

First, we use the method described in Section 5 to obtain the up- and down-going electric wave fields $E^{\pm}(z_r, z_s, p, \tau)$ in the dissipative medium and $\mathscr{E}^{\pm}(z_r, z_s, p, \tau)$ in the effectual medium with a source at z_s and a receiver at z_r. The source and receiver depths of these two datasets are $z_s = -0.76\,\mathrm{m}$ and $z_r = 0\,\mathrm{m}$. The up-going electric field data in the dissipative medium are shown in Fig. 1(a) and displayed with a time-dependent gain of $\exp(0.1 \times \tau)$ to emphasize the later arrivals, here the unit of time is ns. The up-going electric field in the effectual medium is shown in Fig. 1(b). Then we obtain the impulse reflection response $R(z_r, z_r, p, \tau)$ in the dissipative medium and $\mathscr{R}(z_r, z_r, p, \tau)$ in the effectual medium by deconvolution. Fig. 2 shows one trace ($p = 0$) for the impulse reflection response convolved with a 250 MHz Ricker wavelet in the dissipative medium in Fig. 2(a) and in the effectual medium in Fig. 2(b). A time-dependent gain of $\exp(0.1 \times \tau)$ is used to emphasize the later arrivals in Fig. 2(a). We use the data in the dissipative medium and effectual medium to construct the data in the lossless

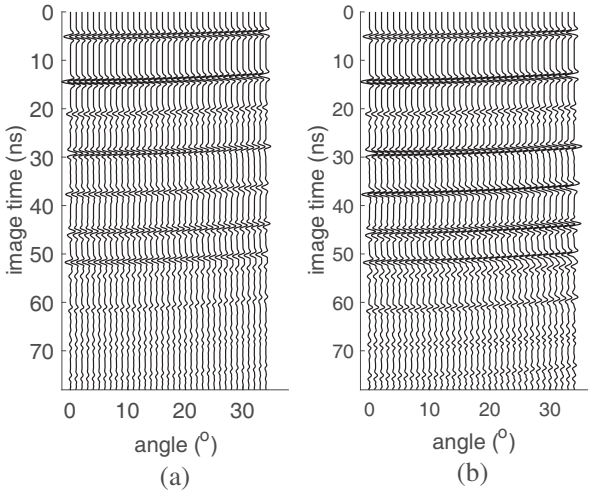

Figure 1. The up-going component of the electric field data as a function of intercept time and incidence angle in the first layer: (a) in the dissipative medium; (b) in the effectual medium.

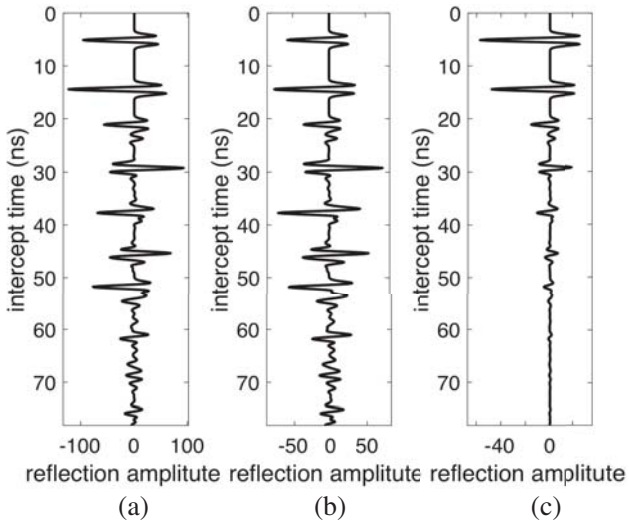

Figure 2. One trace ($p = 0$) for the reflection response: (a) in the dissipative medium, (b) in the effectual medium, and (c) in the lossless medium. The black arrows indicate the primary reflections.

medium shown in Fig. 2(c). The black arrows indicate the primary reflections. Although the multiples are weak in the lossless medium, we still cannot obtain the desired inversion results by directly using the reflection response to implement the inversion scheme by assuming that all events are primary reflections. We shall compare the inversion results later. Once we get the impulse reflection responses in the dissipative medium and effectual medium, these datasets are used in the Marchenko equations to compute the up-going focusing function in both media for all p-values and one-way intercept times until half the maximum recording time. The values of the last event of the up-going focusing function in both media at one-way intercept time are extracted and stored in an image as a function of p. Then we identify the 7 reflectors from the image and pick the image times corresponding to the extrema as a function of the incidence angle for each reflection event. We use their maximum reflection amplitudes in the dissipative medium and the effectual medium to compute the local reflection coefficients in the lossless medium using Eq. (19). Fig. 3 shows the comparison between the estimated local reflection strengths and the expected values as a function of incidence angle for the 2nd reflector in the dissipative medium, effectual medium, and lossless medium. No visible differences occur in the estimated value and expected value.

The following step is that we use the recursive inversion scheme described in Section 6 to compute the permittivity ε and the permeability μ. Starting at the first reflector, Eqs. (20)–(21) are used to find the values of the permittivity ε and the permeability μ in the layered medium and obtain the layer thickness values from the velocities and the one-way travel times.

We then compute the conductivity σ using Eqs. (23)–(24). Here we also compute the inversion results directly using the reflection response by assuming that all events are primary reflections and correct for the transmission effects, then compare them with the Marchenko inversion results (Fig. 4). Fig. 4 shows that Marchenko inversion scheme works well, but the direct inversion scheme does not work. There are two reasons that we cannot use the raw data shown in Fig. 3 to implement inversion scheme directly, even the multiples are very weak. The first reason is that if we assume that every event in Fig. 2 is a primary reflection, the events which actually are multiples would introduce ghost layers. When the multiples were really weak, their presence would be ignored. However, the multiples that are not that weak would lead to incorrect layers and incorrect amplitude corrections leading to incorrect values for ϵ and μ. The second reason is that our inversion scheme is recursive, which means that the accuracy of the former layer inversion result shall influence the next layer inversion result.

The associated errors between the Marchenko inversion results and model values (Table 2) are computed according to following generalized formula err. $= 100(U_{mod} - U_{inv})/U_{mod}$, where U can be ε_r, μ_r, d, or σ, and err. is given in %. The accuracy of the retrieved admittance of each layer is influenced

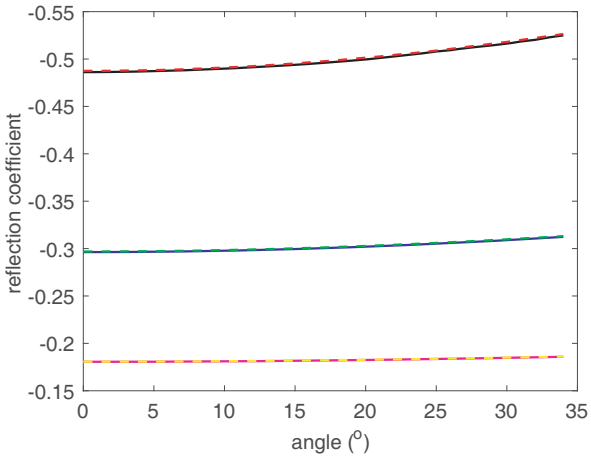

Figure 3. The comparison between the estimated local reflection strengths (solid lines) and the expected values (dashed-dotted lines) as a function of p for the 2nd reflector in the dissipative medium (yellow solid overlaying a dashed-dotted lines), effectual medium (black solid overlaying a dashed-dotted lines) and lossless medium (blue solid overlaying a dashed-dotted lines).

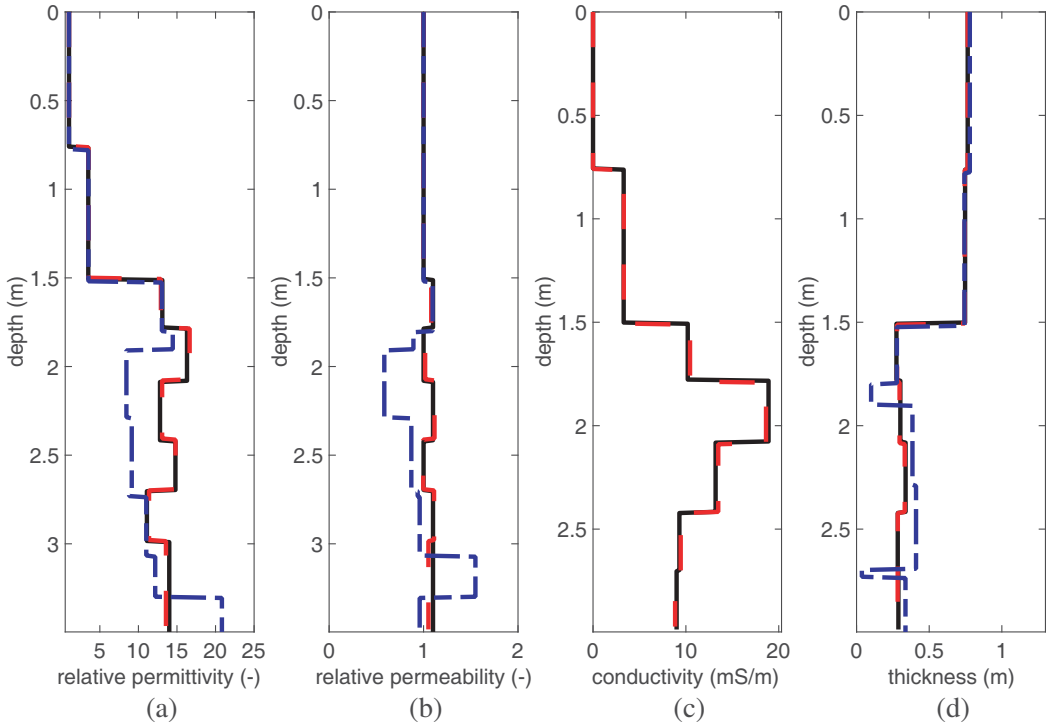

Figure 4. The comparison with the Marchenkon inversion values (red dashed-dotted lines), the direct inversion values (blue dashed-dotted lines) and the model values (solid black lines): (a) relative permittivity; (b) relative permeability; (c) conductivity; and (d) thickness.

by the retrieved reflection coefficient. According to Table 2, the largest relative GRSE of the reflection coefficients occurs in layer 7 which leads to the largest errors of ε_r and μ_r occurring in layer 8 where ε_r is underestimated by 3.07%, and μ_r is underestimated by 4.43%. We compute the thickness based on the velocity in each layer and the one-way travel time leading to the inverse relationship between thickness error and the velocity error or the estimated one-way travel time error. The largest error occurs in

Table 2. The errors for inverted model parameters.

layer	r_{GRSE} (%)	err. (%) $-\varepsilon_r$	err. (%) $-\mu_r$	err. (%) $-\sigma$	err. (%) $-d$
1	-	-	-	-	-
2	0.40	0.63	0.07	1.71	-0.35
3	0.23	-1.41	-1.70	1.70	1.58
4	0.63	2.10	1.65	-2.38	-1.84
5	0.81	2.14	1.44	2.74	-1.75
6	1.33	0.06	-0.34	2.60	0.14
7	2.91	2.51	0.99	-3.03	-1.72
8	0.90	-3.07	-4.43	-	-

the thickness estimation of layer 5, and its thickness is underestimated by 1.84% because the velocity error in this layer is the largest and overestimated. Eqs. (23)–(24) show a complicated relationship between the conductivity and other parameters, which means that the inversion result of conductivity has no simple dependence on the inversion results of the other parameters. The largest error occurs in the conductivity σ of layer 7 which is underestimated by 3.03%. Notice that we do not compute the conductivity and thickness of the last layer due to no reflection signal from the last layer.

Finally, to compute the GRSE of the retrieved dataset for different incidence angles and evaluate the quality of the inversion result, we perform forward modelling using the parameters obtained by the inversion method to compute the reflection data from above and below and compare the results with the model values. The GRSE for the up-going wave fields using the incidence angle from 0° to 34° which are received from above is shown in Fig. 5(a) and the transmission response received from above in Fig. 5(b). The GRSE sharply rises when the incidence angles are larger than 15°. To investigate the

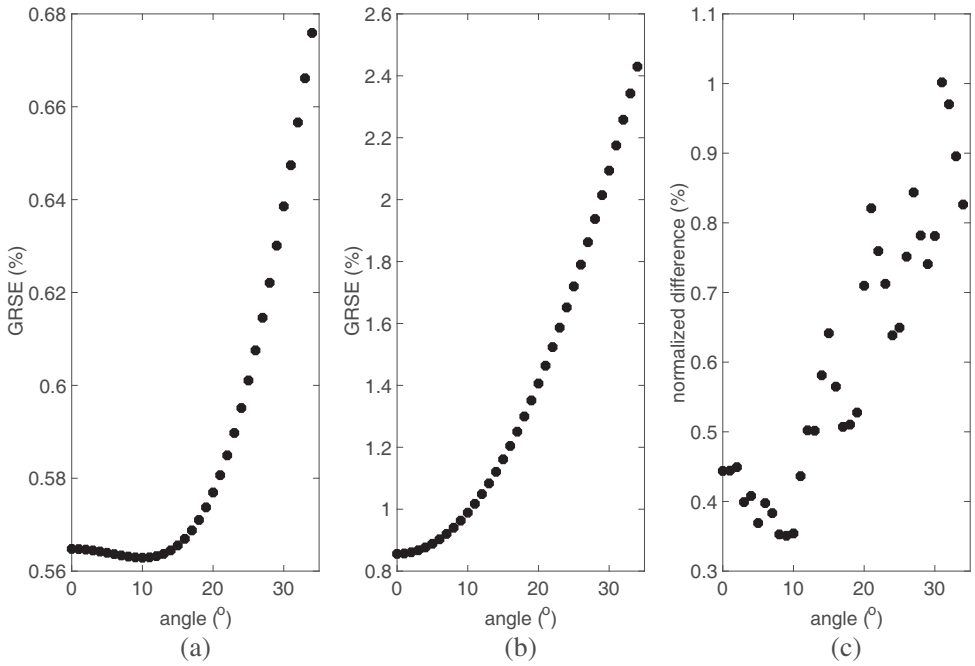

Figure 5. The GRSE of the retrieved dataset for different incidence angles: (a) the GRSE of up-going wave fields received on the surface, (b) the GRSE of transmission data received on the bottom, and (c) The relative errors of the reflection coefficients as a function of p for the 3th reflector in the lossless medium.

reason of this phenomenon, we found that the relative errors of the reflection coefficients for the 3rd reflector in the lossless medium increase when $\varphi > 15°$. The relative errors of the reflection coefficients as a function of p for the 3rd reflector in the lossless medium are shown in Fig. 5(c). It shows that one must take care not to use too large incidence angles because the maximum usable value of p depends on σ and $\sqrt{\varepsilon\mu}$ as we state in Section 2. The GRSE of the up-going wave fields received on the surface for all datasets is 0.59%. The GRSE of the transmission response received at the bottom for all datasets is 1.43%.

7.2. Model with Noise

To investigate the behavior with noisy data, we use the same source and model as above, but add white noise to the data. The noise was implemented in slowness-intercept time domain. To accommodate the effects of additive noise in the actual space-time domain of a measurement, we have used additive and multiplicative noise. The power signal-to-noise ratio (SNR) for per ray parameter is around 40 dB. We model the two-sided measured data with noise in the physical dissipative medium and use the method described in Section 5 to reconstruct data with noise in the effectual medium. We repeat the inversion with 22 different noise realizations, take the average of all inversion results, and compute the standard deviation to quantify the amount of variation or dispersion of the inversion results. The inversion results of the medium parameters and associated errors are shown in Table 3. It can be seen that the largest errors of all parameters occur in layer 6, where the electric permittivity, conductivity, and magnetic permeability are all overestimated. This overestimation is caused by the errors of the retrieved local reflection coefficients. According to Table 3, the errors of the local reflection coefficients, r_{GRSE}, are below 1% but increase sharply to 1.3% and 2.5% after the fifth interface which affects the error of the permittivity and permeability in layer 6. Meanwhile, the layer thickness (interface depth) is underestimated. The largest errors of relative permittivity, relative permeability, conductivity, and

Table 3. The average difference (err. (%)) and standard deviation (STD) for inverted model parameters.

layer	r_{GRSE}	(err., STD) $-\ \varepsilon_r$	(err., STD) $-\ \mu_r$	(err., STD) $-\ c$	(err., STD) $-\ \sigma$	(err., STD) $-\ d$
1	-	-	-	-	-	-
2	0.24	(−0.25, 0.10)	(−0.83, 0.03)	(+0.62, 0.01)	(+0.82, 0.10)	(+0.62, 0.02)
3	0.61	(−4.99, 2.92)	(−5.33, 0.25)	(+9.85, 0.02)	(−2.89, 2.28)	(+9.85, 0.06)
4	0.63	(+2.57, 5.78)	(+2.12, 0.36)	(−5.82, 0.02)	(−1.08, 6.40)	(+5.82, 0.08)
5	1.31	(−0.64, 3.38)	(−1.29, 0.29)	(+7.71, 0.02)	(−0.14, 3.73)	(+7.71, 0.09)
6	2.50	(+9.59, 8.74)	(+9.29, 0.59)	(−7.79, 0.03)	(+11.6, 5.46)	(+7.79, 0.11)
7	1.41	(−2.25, 3.48)	(−3.60, 0.35)	(+12.1, 0.03)	(−5.76, 2.99)	(+12.1, 0.09)
8	-	(+6.53, 16.8)	(+5.29, 1.31)	(−26.5, 0.03)	-	-

Table 4. The errors for inverted model parameters.

layer	err. (%) $-\ \varepsilon_r$	err. (%) $-\ \mu_r$	err. (%) $-\ \sigma$	err. (%) $-\ d$
1	+5.13	−0.87	-	-
2	+3.36	−0.41	+3.95	−1.44
3	−1.06	−3.03	−5.73	+2.10
4	−7.35	−8.63	−2.42	+8.68
5	−4.82	−6.12	−6.21	+5.79
6	−5.26	−5.98	−7.98	+5.95
7	−4.70	−5.60	+4.52	+5.43
8	-	-	-	-

thickness are 9.6%, 9.3%, 11.6%, and 12.1%, respectively. Most of the relatively large errors occur in the last 3 layers. To decrease the errors of these layers, we implement the Marchenko inversion scheme again but from the bottom and up to the first layer. Because the relative permittivity of the bottom layer is 14, the velocity in this layer shall be much smaller than the velocity in the first layer (i.e., the air), and we put the source 0.1 m below the receiver. We use the same method as above to add around 40 dB random white noise to the data and perform the same analysis as above. We take the average of all inversion results and compute the errors between the average values and the model value. The errors for inverted model parameters are shown in Table 4. We observe that due to the noise, the errors of the retrieved local reflection coefficients increase compared with the results of the noise-free model. The inversion scheme shall not work if the noise is too large.

8. CONCLUSION

Electric and magnetic field data measured at two sides of a horizontally layered dissipative medium can be used to create up- and down-going electric fields at one side of the medium and its effectual counterpart. These datasets can be used in the Marchenko redatuming scheme. This scheme gives local reflection coefficients with the attenuation in propagation still present in the dissipative medium. In the effectual medium, the same reflection coefficients are retrieved but with the effectuation in propagation still present. Multiplication of these two results gives information on the reflection coefficients from which electric permittivity and magnetic permeability are retrieved. Division of these results gives information on the attenuation from which the conductivity is retrieved using the obtained permittivity values. Using the computed velocities and arrival times the layer thicknesses are computed. The full waveform inversion is performed by a sequence of linear operations on the data. The numerical example shows that the method is robust for noise levels up to 40 dB of power SNR.

The method is suitable for laminated structures that are accessible on two sides. In the field, it can possibly be used in cross borehole GPR investigations. Extension of the method to 2D and 3D is open for investigation.

ACKNOWLEDGMENT

The financial support for Bingkun Yang was provided by China Scholarship Council (file No. 201609350003).

REFERENCES

1. Amundsen, L., L. T. Ikelle, L. E. Berg, "Multidimensional signature deconvolution and free-surface multiple elimination of marine multicomponent ocean-bottom seismic data," *Geophysics*, Vol. 66, No. 5, 1594–1604, 2001.
2. Benedetto, A. and L. Pajewski, eds., *Civil Engineering Applications of Ground Penetrating Radar*, Springer Transactions in Civil and Environmental Engineering, 2015.
3. Dukalski, M. and K. de Vos, "Marchenko inversion in a strong scattering regime in the presence of a free surface," *Geophys. J Int.*, Vol. 212, No. 2, 760–776, 2018.
4. Ernst, J. R., A. G. Green, H. Maurer, and K. Holliger, "Application of a new 2D time-domain full-waveform inversion scheme to crosshole radar data," *Geophysics*, Vol. 72, No. 5, J53–J64, 2007.
5. Irving J. D. and R. J. Knight, "Removal of wavelet dispersion from ground-penetrating radar data," *Geophysics*, Vol. 68, 960–970, 2003.
6. Kabanikhin, S., "Definitions and examples of inverse and ill-posed problems," *J. Inverse Ill Posed Probl.*, Vol. 16, No. 4, 317–357, 2008.
7. Paige, C. C. and M. A. Saunders, "LSQR: An algorithm for sparse linear equations and sparse least squares," *ACM T. Math. Software*, Vol. 8, No. 1, 43–71, 1982.
8. Ravasi, M., "Rayleigh-Marchenko redatuming for target-oriented, true-amplitude imaging," *Geophysics*, Vol. 82, No. 6, S439–S452, 2017.

9. Slob, E., "Interferometry by deconvolution of multicomponent multioffset GPR data," *IEEE Geosci. Remote Sens.*, Vol. 47, No. 3, 828–838, 2009.
10. Slob, E. and K. Wapenaar, "Coupled Marchenko equations for electromagnetic Green's function retrieval and imaging," *SEG Houston 2013 Annual Meeting*, 1863–1867, Society Exploration Geophysicists, 2013.
11. Slob, E. and K. Wapenaar, "Data-driven inversion of GPR surface reflection data for lossless layered media," *The 8th European Conference on Antennas and Propagation*, 3378–3382, EUCAP, NL, 2014.
12. Slob, E., K. Wapenaar, F. Broggini, and R. Snieder, "Seismic reflector imaging using internal multiples with Marchenko-type equations," *Geophysics*, Vol. 79, No. 2, S63–S76, 2014.
13. Slob, E., "Green's function retrieval and marchenko imaging in a dissipative acoustic medium," *Phys. Rev. Lett.*, Vol. 116, No. 16, 1–6, 2016.
14. Slob, E. and K. Wapenaar, "Theory for marchenko imaging of marine seismic data with free surface multiple eliminationg," *79th EAGE Conference & Exhibition*, A1–A4, EAGE, NL, 2017.
15. Slob, E., "Theory for 1D full waveform inversion of surface GPR data," *17th International Conference on Ground Penetrating Radar*, 306–309, Institute of Electrical and Electronics Engineers Inc., 2018.
16. Tarantola, A., *Inverse Problem Theory and Methods for Model Parameter Estimation*, Society for Industrial and Applied Mathematic, 2005.
17. Van Der Neut, J. and J. T. Fokkema, "One-dimensional marchenko inversion in stretched space," *Proceedings of the International Workshop on Medical Ultrasound Tomography*, 15–24, T. Hopp, N. Ruiter, J. C. Bamber, N. Duric, and K. W. A. van Dongen, Eds., 2017.
18. Wapenaar, C., M. Dillen, and J. T. Fokkema, "Reciprocity theorems for electromagnetic or acoustic one-way wave fields in dissipative inhomogeneous media," *Radio Sci.*, Vol. 36, No. 5, 851–863, 2001.
19. Wapenaar, K., J. Thorbecke, J. Van Der Neut, F. Broggini, E. Slob, and R. Snieder, "Marchenko imaging," *Geophysics*, Vol. 79, No. 3, WA39–WA57, 2014.
20. Yang, B. and E. Slob, "Theory for 1D GPR data inversion for a dissipative layered medium," *17th International Conference on Ground Penetrating Radar*, 302–305, Institute of Electrical and Electronics Engineers Inc., 2018.
21. Yang, X., A. Klotzsche, G. Meles, H. Vereecken, and J. Van Der Kruk, "Improvements in crosshole GPR full-waveform inversion and application on data measured at the Boise Hydrogeophysics Research Site," *J. Appl. Geophys.*, Vol. 99, 114–124, 2013.